PTF 11kx: a type Ia supernova with a symbiotic nova progenitor — **Source link** ↗

Ben Dilday, Ben Dilday, D. A. Howell, D. A. Howell ...+38 more authors

Institutions: Las Cumbres Observatory Global Telescope Network, University of California, Santa Barbara, University of California, Berkeley, Lawrence Berkeley National Laboratory ...+15 more institutions

Topics: Supernova, RS Ophiuchi and White dwarf

Related papers:

- Detection of Circumstellar Material in a Normal Type Ia Supernova

- Binaries and Supernovae of Type I

- Double white dwarfs as progenitors of R Coronae Borealis stars and type I supernovae

- An asymptotic-giant-branch star in the progenitor system of a type Ia supernova.

- Supernovae of type I as end products of the evolution of binaries with components of moderate initial mass (M< or approx. =9 M/sub sun/)

PTF 11kx: A Type-Ia Supernova with a Symbiotic Nova Progenitor

B. Dilday[1,2*], D. A. Howell[1,2], S. B. Cenko[3], J. M. Silverman[3], P. E. Nugent[3,4],
M. Sullivan[5], S. Ben-Ami[6], L. Bildsten[2,7], M. Bolte[8], M. Endl[9], A. V. Filippenko[3],
O. Gnat[10], A. Horesh[12], E. Hsiao[4,11], M. M. Kasliwal[12,13], D. Kirkman[14],
K. Maguire[5], G. W. Marcy[3], K. Moore[2], Y. Pan[5], J. T. Parrent[1,15],
P. Podsiadlowski[5], R. M. Quimby[16], A. Sternberg[17], N. Suzuki[4], D. R. Tytler[14],
D. Xu[6], J. S. Bloom[3], A. Gal-Yam[18], I. M. Hook[5],
S. R. Kulkarni[12], N. M. Law[19], E. O. Ofek[18], D. Polishook[20], D. Poznanski[21]

[1]Las Cumbres Observatory Global Telescope Network, 6740 Cortona Dr., Suite 102, Goleta, California 93117, USA

[2]Department of Physics, University of California, Santa Barbara, Broida Hall, Mail Code 9530, Santa Barbara, California 93106-9530, USA

[3]Department of Astronomy, University of California, Berkeley, CA 94720-3411, USA

[4]Lawrence Berkeley National Laboratory, Mail Stop 50B-4206, 1 Cyclotron Road, Berkeley, California 94720, USA

[5]Department of Physics (Astrophysics), University of Oxford, Keble Road, Oxford, OX1 3RH, UK

[6]Department of Particle Physics and Astrophysics, The Weizmann Institute of Science, Rehovot 76100, Israel

[7]Kavli Institute for Theoretical Physics, University of California, Santa Barbara, CA, 93106, USA

[8]UCO/Lick Observatory, University of California, Santa Cruz, California 95064, USA

[9]McDonald Observatory, The University of Texas at Austin, Austin, TX 78712, USA

[10]Racah Institute of Physics, The Hebrew University of Jerusalem, 91904, Israel

[11]Carnegie Institution of Washington, Las Campanas Observatory, Colina El Pino, Casilla 601, Chile

[12]Cahill Center for Astrophysics, California Institute of Technology, Pasadena, CA, 91125, USA

[13]Observatories of the Carnegie Institution for Science, 813 Santa Barbara St, Pasadena CA 91101 USA

[14]Center for Astrophysics and Space Sciences, University of California San Diego, La Jolla, CA 92093-0424, USA

[15]Department of Physics and Astronomy, Dartmouth College, Hanover, NH, USA

[16]IPMU, University of Tokyo, 5-1-5 Kashiwanoha, Kashiwa-shi, Chiba, 277-8583, Japan

[17]Minerva Fellow, Max Planck Institute for Astrophysics, Karl Schwarzschild St. 1, D-85741 Garching, Germany

[18]Benoziyo Center for Astrophysics, The Weizmann Institute of Science, Rehovot 76100, Israel

[19]University of Toronto, 50 St. George Street, Toronto M5S 3H4, Ontario, Canada

[20]Department of Earth, Atmospheric, and Planetary Sciences, Massachusetts Institute of Technology, Cambridge, MA 02139, USA

[21]School of Physics and Astronomy, Tel-Aviv University, Tel-Aviv 69978, Israel

*To whom correspondence should be addressed. E-mail: bdilday@lcogt.net

2

There is a consensus that Type-Ia supernovae (SNe Ia) arise from the thermonuclear explosion of white dwarf stars that accrete matter from a binary companion. However, direct observation of SN Ia progenitors is lacking, and the precise nature of the binary companion remains uncertain. A temporal series of high-resolution optical spectra of the SN Ia PTF 11kx reveals a complex circumstellar environment that provides an unprecedentedly detailed view of the progenitor system. Multiple shells of circumsteller are detected and the SN ejecta are seen to interact with circumstellar material (CSM) starting 59 days after the explosion. These features are best described by a symbiotic nova progenitor, similar to RS Ophiuchi.

Supernova PTF 11kx was discovered January 16, 2011 (UT) by the Palomar Transient Factory (PTF), at a cosmological redshift of $z = 0.04660 \pm 0.00001$ (*1*). This corresponds to a luminosity distance of ~ 207 Mpc. The initial spectrum of PTF 11kx, taken January 26, 2011, showed saturated absorption in the Ca II H&K lines, along with weak absorption in the Na I D lines (Fig. 1). In interstellar gas, the Na I D lines are usually of strength comparable to (or greater than) that of the Ca II lines (*2*); thus, this combination of absorption features indicated that PTF 11kx may have affected its surroundings, revealing evidence of its circumstellar environment and progenitor system. SNe Ia are known to exhibit photometric (*3, 4*) and spectroscopic (*5*) diversity that is correlated with intrinsic brightness, such that bright (faint) SNe Ia have relatively broad (narrow) light curves, high (low) photospheric temperature, and weak (strong) Si II $\lambda6150$ absorption. Aside from the saturated Ca II absorption, the initial spectrum and a subsequent temporal series of spectra show PTF 11kx to resemble SN 1999aa (*6, 7*), a broad/bright SN Ia (Fig. 1). This suggests that insights into the progenitor of PTF 11kx may be applicable to SNe Ia generally, rather than to only a subset of peculiar objects. A complete sample of nearby SNe Ia shows that the subclass similar to SN 1999aa comprises $\geq 9\%$ of all

SNe Ia (*8*).

We obtained high-resolution spectra ($R \approx 48,000$) of PTF 11kx with the Keck I High Resolution Echelle Spectrometer (HIRES) instrument at -1, $+9$, $+20$, and $+44$ days, relative to B-band maximum light. Low-resolution spectra were obtained on 14 epochs between -3 and $+130$ days and show the composition and evolution of features that are unique to SNe Ia (Fig. 1). The SN system is blueshifted from the galaxy cosmological redshift by ~ 100 km s^{-1}, as determined from the strongest narrow interstellar Na D absorption line (*9, 10*). An assumption that emission lines from a nearby H II region evident in the two-dimensional spectra are indicative of the progenitor velocity gives a consistent result.

The high-resolution spectra reveal narrow absorption lines of Na I, Fe II, Ti II, and He I (Fig. 2). All are blueshifted by a velocity of ~ 65 km s^{-1} relative to the progenitor system, with a velocity dispersion of ~ 10 km s^{-1}, and are consistent with arising in the same cloud or shell. The sodium lines increase in depth over time, a feature which has been resolved in high-resolution spectra of two previous SNe Ia (SN 2006X and SN 2007le), and has been explained as the photoionization of CSM by the SN light, followed by recombination that is detected through the increased presence of neutral sodium (*9,11*). A statistical study using high-resolution spectra of 35 SNe Ia has shown that at least 20% of those with spiral host galaxies have circumstellar material revealed through narrow Na I D absorption lines (*10*).

However, narrow lines of circumstellar Fe II, Ti II, and He I have not been seen previously in a SN Ia. He I $\lambda5876$ strengthens over time, which can be explained by photoionization and recombination, if sufficient far-ultraviolet (UV) photons are generated in the early phases of the SN. SNe Ia are expected to produce only weak emission in the far-UV, but interaction of the SN ejecta with an extended progenitor such as a red giant star can produce an excess of X-ray and UV photons (*12*). Lower excitation states of Fe II $\lambda\lambda4923$, 5018, 5169 decrease in strength in time, while higher excitation states such as Fe II $\lambda5316$ remain constant. A possible explanation

for this is that the excitation energy of Fe II λ5316 (3.153 eV) corresponds to the saturated Ca II K line, and thus the population of this level is unaffected by the SN light. Because SNe Ia are weak sources in the UV, the distance over which they can ionize gas is limited, and hence the observed photoionization indicates that the material is circumstellar (*9, 11*). An alternative explanation, as the projection effect of different interstellar clouds, was proposed for the time-variable Na I D lines in SN 2006X (*13*); however, interaction with the CSM in PTF 11kx demonstrates conclusively that CSM is present. There are other narrow sodium features at different relative velocities that do not vary with time, which must originate at a larger distance and are most likely interstellar (Fig. 2).

The hydrogen Balmer series is clearly detected in absorption at ~ 65 km s^{-1}, and is consistent with being at the same velocity as the Fe II, Ti II, Na I, and He I lines (Fig. 2). The Hα and Hβ lines show narrow P-Cygni profiles, which are characteristic of an expanding shell of radiating material. The presence of circumstellar hydrogen has long been identified as one of the characteristics expected in the single-degenerate SN Ia progenitor model (*14, 15*), but has only been detected in at most two other cases, SN 2002ic (*16*) and SN 2005gj (*17*), and only at levels much stronger than in the early epochs of PTF 11kx.

These narrow features of H, He, Fe, Ti, and Na arise from material that is distinct from the stronger Ca absorption, which, owing to its more blueshifted absorption minimum of ~ 100 km s^{-1}, must be at a higher velocity. In fact, at later epochs, emission lines of Ca and H emerge, marking the onset of interaction between SN ejecta and CSM. This transition of circumstellar lines from absorption to emission has not previously been observed in a SN Ia, and shows definitively the presence of CSM. Narrow absorption components can be seen atop the broader emission (FWHM ≈ 1000 km s^{-1}; Fig. 3), indicating that there are two regimes of material, with the faster-moving H and Ca interior to the slower-moving shell (Fig. 4.)

The saturation of the Ca II K line near maximum light requires that no part of the SN

5

photosphere is uncovered by the absorbing material; this constrains the distance of the absorbing cloud from the progenitor to be further than the SN ejecta, and the size of the cloud to be as large as the SN photosphere. Assuming typical values for the ejecta expansion velocity of the outer layers of the exploding white dwarf of 25,000 km s^{-1}, and mean photospheric velocity of 10,000 km s^{-1}, these constraints are $\sim 4.3 \times 10^{15}$ cm and $\sim 1.7 \times 10^{15}$ cm, respectively (Fig. 4). The column density of Ca II in the near-maximum-light spectra is determined to be $\sim 5 \times 10^{18}$ cm^{-2} (*18*). Assuming that the Ca is part of a spherical shell of material with uniform density would imply a total mass in the CSM (~ 5.3 M$_\odot$) which is incompatible with the photometric behavior of the SN (*18*). Therefore, the material must be non-uniform. A small range of viewing angles that intersect such a dense cloud of absorbing material may partly explain the rare occurrence of variable absorption features in SNe Ia.

The Ca II H&K lines detected in lower resolution spectra confirm the disappearance of the absorption over ~ 40 days and the emergence of a broad emission feature in the spectrum taken +39 days after maximum (Fig. 1). The broad emission feature initially exhibits a narrower absorption component as well (possibly because of an outer shell of CSM; Fig. 4), but this is no longer evident after day +56. At day +39, Hα also begins to exhibit a broad emission component. Assuming a rise time of ~ 20 days and an ejecta velocity of 25,000 km s^{-1} would imply that the location of the interaction is $\sim 10^{16}$ cm. The temporal evolution of the Ca II K and Hα lines are shown in Fig. 3.

A model for the progenitor of PTF 11kx must thus explain the presence of multiple components of CSM, fast-moving material interior to slower moving material, velocities of the narrow absorption components that are larger than typical red giant winds, and a region evacuated of CSM, leading to a delay between explosion and the emergence of broad components of Ca and H emission. A SN Ia occurring in a symbiotic nova system naturally provides an explanation for all of these features. In this model, accretion onto a near-Chandrasekhar-mass white dwarf

6

occurs through the wind from a red giant star. The wind also deposits CSM into the system which is concentrated in the orbital plane (*19*). Episodic thermonuclear runaways on the surface of the white dwarf cause nova events, which eject a mass of $\sim 10^{-7}$ $M_\odot$ at velocities of thousands of km s^{-1}. This process results in expansion velocities of CSM at ~ 50–100 km s^{-1} concentrated in the orbital plane, as is observed in high-resolution spectra of RS Ophiuchi (*20*). The delay in the interaction between SN ejecta and CSM, leading to the emergence of the broad Hα and Ca II emission, is explained as being due to an evacuated region around the SN caused by the previous nova event (*21*) that will be present until the red giant wind has had time to replenish the local CSM.

The system of features seen in the spectra of PTF 11kx is inconsistent with expectations for double-degenerate SN Ia progenitors. Double-degenerate SN Ia progenitors first go through a common-envelope phase where the outer layers of the secondary are stripped, resulting in large amounts of CSM. However, it is generically expected that the envelope material will have dissipated by the time of the SN Ia event (*22*). Recent modeling of the white dwarf merger process in double-degenerate SN models suggests that heating in the accretion disk can drive a wind, depositing CSM into the system; however, because of the previous common-envelope phase, the presence of hydrogen cannot be accounted for (*23*). Alternative models for SN 2002ic and SN 2005gj which suggested that they were not SNe Ia are also implausible for PTF 11kx (*18*).

For epochs less than ~ 20 days after maximum, the light curve of PTF 11kx resembles that of typical broad/bright SNe-Ia (*18*). Using the color law of the SiFTO (*24*) light-curve model, we estimate that PTF 11kx is only moderately extinguished by dust (~ 0.5 mag in V), and that the absolute magnitude ($M_V \approx -19.3$) is as expected for a SN 1999aa-like SN Ia. At epochs later than ~ 20 days, the light curve appears brighter than the SN Ia templates, indicating that some brightening due to CSM interaction has begun. At an epoch of $\sim +280$ days the SN is

at an absolute magnitude of ~ -16.6, roughly 3 mag brighter than expected, indicating that circumstellar interaction is still ongoing. Circumstellar interaction, including broad H emission and excess luminosity, was observed previously in SN 2002ic and SN 2005gj, which had the appearance of the extreme broad/bright SN 1991T, superposed with features from strong CSM interaction. The strength of the interaction casts some doubt on their identity as SNe Ia, which is not the case for PTF 11kx (Fig. 1). Indeed, PTF 11kx bridges the observational gap between broad/bright SNe Ia and SN 2002ic/SN 2005gj, showing that SNe Ia exist with CSM interaction that is weaker and begins much later after explosion. This supports and enhances the interpretation that the earlier SNe with H emission were SNe Ia, where the strength of the CSM interaction depends on details of the progenitor system, such as the mass-loss and accretion rates and the time since the last nova eruption.

Measurements of the host-galaxy properties for SNe Ia suggest that broad/bright SNe Ia arise from relatively young stellar populations (*25*), and a complete understanding of SN Ia progenitors must account for the occurrence of CSM interaction preferentially in young progenitor systems (*10*). The host galaxy of PTF 11kx is a spiral galaxy with active star formation, and therefore has a substantial fraction of young stars. In contrast to SN 2002ic/SN 2005gj, the host galaxy has typical values for mass and metallicity, so there is no evidence that PTF 11kx must have come from an atypical stellar population.

There are several indications that white dwarf mergers are required to explain some SNe Ia, including the rate in old stellar populations (*26*) and the existence of SNe Ia radiating at a luminosity that requires an exploding white dwarf above the Chandrasekhar limit (*27, 28*). The lack of a surviving companion near the remnant of a SN Ia in the Large Magellanic Cloud has provided evidence for a double-degenerate progenitor for that particular case (*29*). A symbiotic nova progenitor has been ruled out for the nearby SN Ia PTF11kly/SN 2011fe (*30*), which implies either a main sequence companion or a double-degenerate progenitor (*31, 32*). On the

other hand, the detection of CSM, inferred through either temporal variability (*9, 11*) or statistical analysis of the velocity (*10*) of narrow absorption features, has provided recent evidence in support of the single-degenerate progenitor scenario for some SNe Ia. The remnant of Kepler's SN shows evidence for interaction with a circumstellar shell which supports a single-degenerate progenitor for that SN Ia (*33*).

The system of features observed in PTF 11kx supplies direct evidence for a single-degenerate progenitor with a red giant companion, and our data suggest a link between SNe Ia that show weaker signatures of the circumstellar environment (SN 2006X, SN 2007le, Kepler's SN) and those that show stronger signatures (SN 2002ic, SN 2005gj). The fraction of SNe Ia that exhibit prominent circumstellar interaction near maximum light is $\sim$ 0.1–1%, but more subtle indications of a symbiotic progenitor could be missed in typical SN observations (*18*). Additionally, even more extreme interaction of a SN Ia with CSM would not be distinguishable from a Type IIn SN, and it has been speculated that some SNe IIn are in fact SNe Ia hidden within very strong CSM interaction (*16*). Our data imply that there is indeed a wide range of CSM interaction possible from SNe Ia, and support this interpretation. If this is the case, then current estimates of the rate of SNe with progenitors similar to that of PTF 11kx will be underestimated. Theoretical expectations for the fraction of SNe Ia from the symbiotic progenitor channel are $\sim$ 1–30% (*34, 35*), consistent with observational constraints.

The solution to the long-standing puzzle of the progenitors of SNe Ia is that there is no single progenitor path. It remains to be determined in what proportion different progenitor channels contribute to the total rate of SNe Ia, whether different channels result in different absolute luminosities or color evolution, and how the potential change of the relative contributions of different channels with look-back time may affect the use of SNe Ia in accurately measuring cosmological expansion.

References and Notes

1. H. Aihara, *et al.*, *ApJS* **193**, 29 (2011).

2. D. E. Welty, D. C. Morton, L. M. Hobbs, *ApJS* **106**, 533 (1996).

3. I. P. Pskovskii, *Soviet Ast.* **21**, 675 (1977).

4. M. M. Phillips, *ApJ* **413**, L105 (1993).

5. P. Nugent, M. Phillips, E. Baron, D. Branch, P. Hauschildt, *ApJ* **455**, L147 (1995).

6. W. Li, *et al.*, *ApJ* **546**, 734 (2001).

7. G. Garavini, *et al.*, *AJ* **128**, 387 (2004).

8. W. Li, *et al.*, *MNRAS* **412**, 1441 (2011).

9. F. Patat, *et al.*, *Science* **317**, 924 (2007).

10. A. Sternberg, *et al.*, *Science* **333**, 856 (2011).

11. J. D. Simon, *et al.*, *Astrophys. J.* **702**, 1157 (2009).

12. D. Kasen, *ApJ* **708**, 1025 (2010).

13. N. N. Chugai, *Astronomy Letters* **34**, 389 (2008).

14. I. Iben, Jr., A. V. Tutukov, *ApJS* **54**, 335 (1984).

15. D. Branch, M. Livio, L. R. Yungelson, F. R. Boffi, E. Baron, *PASP* **107**, 1019 (1995).

16. M. Hamuy, *et al.*, *Nature* **424**, 651 (2003).

17. G. Aldering, *et al.*, *ApJ* **650**, 510 (2006).

18. Additional information is available in the supplementary materials.

19. R. Walder, D. Folini, S. N. Shore, *A&A* **484**, L9 (2008).

20. F. Patat, *et al.*, *A&A* **530**, A63+ (2011).

21. W. M. Wood-Vasey, J. L. Sokoloski, *ApJ* **645**, L53 (2006).

22. N. N. Chugai, *et al.*, *MNRAS* **352**, 1213 (2004).

23. K. J. Shen, L. Bildsten, D. Kasen, E. Quataert, *ApJ* **748**, 35 (2012).

24. A. Conley, *et al.*, *ApJ* **681**, 482 (2008).

25. M. Sullivan, *et al.*, *ApJ* **648**, 868 (2006).

26. D. Maoz, K. Sharon, A. Gal-Yam, *ApJ* **722**, 1879 (2010).

27. D. A. Howell, *et al.*, *Nature* **443**, 308 (2006).

28. J. M. Silverman, *et al.*, *MNRAS* **410**, 585 (2011).

29. B. E. Schaefer, A. Pagnotta, *Nature* **481**, 164 (2012).

30. W. Li, *et al.*, *Nature* **480**, 348 (2011).

31. P. E. Nugent, *et al.*, *Nature* **480**, 344 (2011).

32. A. Horesh, *et al.*, *ApJ* **746**, 21 (2012).

33. A. Chiotellis, K. M. Schure, J. Vink, *A&A* **537**, A139 (2012).

34. Z. Han, P. Podsiadlowski, *MNRAS* **350**, 1301 (2004).

35. G. Lü, C. Zhu, Z. Wang, N. Wang, *MNRAS* **396**, 1086 (2009).

36. N. M. Law, *et al.*, *PASP* **121**, 1395 (2009).

37. A. Rest, *et al.*, *ApJ* **634**, 1103 (2005).

38. G. Miknaitis, *et al.*, *ApJ* **666** (2007).

39. A. C. Becker, *et al.*, *ApJ* **611**, 418 (2004).

40. P. L. Schechter, M. Mateo, A. Saha, *PASP* **105**, 1342 (1993).

41. H. Aihara, *et al.*, *ApJS* **193**, 29 (2011).

42. A. Conley, *et al.*, *ApJ* **681**, 482 (2008).

43. M. Turatto, S. Benetti, E. Cappellaro, *From Twilight to Highlight: The Physics of Supernovae*, W. Hillebrandt & B. Leibundgut, ed. (2003), p. 200.

44. D. Poznanski, M. Ganeshalingam, J. M. Silverman, A. V. Filippenko, *MNRAS* **415**, L81 (2011).

45. S. Jha, A. G. Riess, R. P. Kirshner, *ApJ* **659**, 122 (2007).

46. J. A. Holtzman, *et al.*, *AJ* **136**, 2306 (2008).

47. N. Panagia, *et al.*, *ApJ* **646**, 369 (2006).

48. F. Patat, *et al.*, *A&A* **530**, A63+ (2011).

49. C. A. Tremonti, *et al.*, *ApJ* **613**, 898 (2004).

50. I. Iben, Jr., A. Renzini, *ARA&A* **21**, 271 (1983).

51. C. Trundle, R. Kotak, J. S. Vink, W. P. S. Meikle, *A&A* **483**, L47 (2008).

52. Benetti, S., *et al.*, ApJ, **653**, L129 (2006).

53. Livio, M. & Riess, A. G., ApJ, **594**, L93 (2003).

54. Han, Z. & Podsiadlowski, P., MNRAS, **368**, 1095 (2006).

55. Dilday, B., *et al.*, ApJ, **713**, 1026 (2010).

56. Eck, C. R., Cowan, J. J., & Branch, D., ApJ, **573**, 306 (2002).

57. S. S. Vogt, *et al.*, *Society of Photo-Optical Instrumentation Engineers (SPIE) Conference Series*, D. L. Crawford & E. R. Craine, ed. (1994), vol. 2198 of *Society of Photo-Optical Instrumentation Engineers (SPIE) Conference Series*, p. 362.

Supplementary Material

S1. Spectroscopy

Optical spectra of PTF 11kx were obtained with several different telescopes: the Lick 3 m, Palomar 5 m, KPNO 4 m, WHT, Keck, and Gemini North. Spectra from the High Resolution Echelle Spectrometer (HIRES) on Keck I were reduced using the Mauna Kea Echelle Extraction (`makee`) software package[1]. Spectra from other telescopes and instruments were reduced using standard methods. Journals of observations are given in Tables S1 and S2; UT dates are used throughout this paper. A time series of low-resolution spectra for PTF 11kx is shown in Fig. 1.

S2. Photometry

Photometry in the r band was collected as part of the normal PTF transient search on the Palomar 48 in telescope (*36*). PTF 11kx was also followed by the 2 m Faulkes Telescope North. Between January 27, 2011 and June 9, 2011 (133 days), 46 epochs were obtained in the SDSS g and r bands, and 45 epochs in the SDSS i band. Photometric observations of PTF 11kx were resumed on September 30, 2011. At the location of PTF 11kx there is a substantial background due to the host galaxy. When this is the case, photometry for SNe is usually accomplished through difference imaging analysis, where an image without the SN present is used as a difference imaging template. Reference images for PTF 11kx have not yet been taken on the Faulkes North, and so only preliminary photometry is currently available. To at least roughly subtract the host galaxy, we used SDSS images as difference imaging templates. Visual inspection of the difference images reveals that the host-galaxy background is subtracted successfully, and

---

[1]http://spider.ipac.caltech.edu/staff/tab/makee

thus the use of templates from a different instrument does not significantly affect the conclusions that PTF 11kx is a member of the broad/bright SN class. Initial photometry suggests that PTF 11kx declines more slowly at epochs later than $\sim +20$ days than the templates of the same class, which is another indication of circumstellar interaction, and late-time (~ 280 days) photometry confirms this. Data were processed using the `photpipe` reduction pipeline (*37, 38*). Difference imaging was done using `hotpants` (*39*). Source detection and PSF photometry was done using `dophot` (*40*). The photometry was calibrated by comparison of stars in the field of PTF 11kx to magnitudes provided by the SDSS DR8 database (*41*).

S3. SN Light Curve

Comparing the colors of the SN to templates from the SiFTO SN light-curve model (*42*), we estimate that the SN is only moderately extinguished by dust, with the extinction amounting to ~ 0.5 mag in the V band. It is commonly assumed that the equivalent width of the Na D lines is correlated with the value for extinction by dust (e.g. *43*), and so the small value of the equivalent width of the non-variable Na D lines also supports this conclusion. While this correlation has been shown to have significant scatter (*44*), this is most relevant for equivalent widths larger than those measured in PTF 11kx. Assuming a concordance cosmology ($H_0 = 70$ km s^{-1} Mpc^{-1}), the absolute B-band magnitude of PTF 11kx is ~ -19.3, which is on the bright end of the SN Ia luminosity function and is consistent with the observed distribution of high-stretch SNe Ia. The date of maximum light (in the B band) of PTF 11kx is January 29, 2011. Comparisons with the broad SN Ia 1999aa (*45*), the "normal" SN Ia 2002er (*45*), and the CSM-interaction SNe Ia 2002ic (*17*) and 2005gj (*46*), are shown in Fig. S1. While the photometry is preliminary, we can draw a few important conclusions: (i) the light curve is of the high-stretch class and is qualitatively similar to that of SN 1999aa and SN 1991T, (ii) the

15

light curve is markedly dissimilar to that of SN 2002ic and SN 2005gj, and (iii) the absolute magnitude at peak is consistent with the population of previously observed SNe Ia.

S4. Radio Observation

PTF 11kx was observed on March 30, 2011 in the X-band using the Expanded Very Large Array (EVLA), yielding a nondetection with a 1σ root-mean-square of 23 μJy. Using a model of SN interaction with a smooth wind puts an upper limit on the inferred mass-loss rate in the wind (*47*) of $\sim 4.5 \times 10^{-6}$ M$_\odot$ yr^{-1} ($v_{\rm w}$/10 km s^{-1})$^{1.65}$, where $v_{\rm w}$ is the velocity of the wind. The radio emission strength depends on microphysical parameters such as the strength of the magnetic fields generated in the interaction (the ϵ_B parameter), and if these magnetic fields are weaker than has generally been assumed, then the constraints on the rate of mass loss would be less strict by perhaps an order of magnitude (*31*). Estimates of the mass-loss rate for symbiotic novae such as RS Ophuichi are $\sim 3 \times 10^{-7}$ M$_\odot$ yr^{-1}, well below our constraint (*48*).

S4. Host-Galaxy Properties

The host galaxy of PTF 11kx is a late-type, spiral galaxy. The properties of the host galaxy, such as the star-formation rate, mass, and metallicity, are not unusual in any way. The absolute magnitude is $M_g \approx -19.47$, and the metallicity has been derived by (*49*) to be 12 + log(O/H) ≈ 8.93, which is slightly larger than solar. This indicates that PTF 11kx does not obviously arise from an atypical local environment. As a comparison, the host galaxies for SN 2002ic and SN 2005gj were low-luminosity galaxies with corresponding low metallicities, which has been assumed to play a role in the presence of CSM in the SN systems. PTF 11kx demonstrates that CSM interaction can occur in a SN Ia even in a more normal galactic environment.

S5. Alternative Models for CSM-Interaction SNe Ia

As discussed in the main text, PTF 11kx bears similarities to SN 2002ic, an apparent SN Ia with circumstellar interaction. Subsequent to the discovery of SN 2002ic, several alternative models were proposed as possible explanations. Given the association of PTF 11kx with SN 2002ic we question whether any of those models are viable alternatives for PTF 11kx. In PTF 11kx, the multiple shells of CSM, the nonuniform distribution of the CSM, and the long delay between explosion and circumstellar interaction are important additional constraints.

The "SN 1.5" Model: The "SN 1.5" model involves the explosion of the degenerate core of a massive star (*50*). This model cannot explain the long delay in the onset of emission, the nonuniform distribution of CSM, or the multiple shells of material seen in PTF 11kx.

A Luminous Blue Variable Progenitor: The arguments for an LBV progenitor applied only to SN 2005gj (*51*), which had much stronger CSM interaction than SN 2002ic, and were based mainly on the double P-Cygni profile in the Hα line, a feature which is not present in PTF 11kx.

A Peculiar SN Ic: The possibility that SN 2002ic was a SN Ic (*52*) was based on the possible presence of Mg and O in the late-time spectra. The spectra of PTF 11kx shown in Fig. 1 definitively rule out a core-collapse SN in this case.

A Double-Degenerate SN Ia: Subsequent to the suggestion that SN 2002ic had a double-degenerate progenitor (*53*), additional modeling has shown that it is not expected that any significant circumstellar material from the common-envelope phase can remain at the time of the

SN explosion (*22*). Moreover, modeling of the possible CSM due to wind generated during the merger process of a double-degenerate progenitor cannot account for the presence of hydrogen (*23*). A double-degenerate progenitor also does not explain the multiple distinct shells of CSM.

Supersoft, Single-Degenerate Progenitor: The model of (*54*) could possibly explain many of the features of PTF 11kx, but our symbiotic nova model naturally explains the low expansion velocity of the CSM (65 km s^{-1} for PTF 11kx instead of ~ 100 km s^{-1}), the multiple shells of CSM, and the delay between explosion and interaction, while the (*54*) model does not.

S6. Rate of SNe Ia with Symbiotic Nova Progenitors

One of the features of PTF 11kx that supports the conclusion that it is from a symbiotic nova progenitor is the prominent H and Ca emission seen ~ 59 days after explosion. The SDSS-II SN Survey had a high degree of spectroscopic completeness for SNe Ia at $z < 0.15$, and the discovery of one CSM-interaction SN Ia (SN 2005gj) in a sample of 80 SNe Ia with $z < 0.15$ implies a rate of such SNe of $\sim 1\%$ (*55*). The Palomar Transient Factory currently has discovered ~ 1000 SNe Ia with one known example of a CSM-interaction SN Ia (PTF 11kx), but the spectroscopic completeness has not yet been determined or quantified and so this can only be considered an order of magnitude estimate for the rate of CSM-interaction SNe.

However, an important conclusion from the discovery of PTF 11kx is that SNe Ia exist that show CSM-interaction at weaker levels and later onset than SN 2002ic and SN 2005gj. This suggests that there is a continuum of CSM-interaction in SNe Ia. If the continuum of interaction strength extends to lesser values and later onsets, then the signs of interaction would be missed in a large fraction of SNe Ia, as they do not typically have high-signal-to-noise ratio spectroscopic observations at epochs > 60 days after explosion. The discovery of PTF 11kx

18

highlights the importance of more extensive spectroscopic and photometric follow-up monitoring for SNe Ia extending to late times to determine the rate of SNe Ia with significant circumstellar material from the progenitor system. Furthermore, CSM-interaction SNe Ia with greater interaction strength could be classified as SNe IIn and these would contribute an undetermined fraction to the overall SN Ia rate. Therefore, we can only say that SNe Ia with prominent CSM interaction occurring near maximum light is ~ 0.1–1%. Population synthesis modeling predicts the fraction of SNe Ia from the symbiotic binary channel to be $\sim 1\%$ (*33*) to as much as 30% (*34*), which encompasses the range of observational constraints.

The existence of a red giant companion could in principle be detected through radio emission due to interaction of the SN ejecta with the wind from the secondary, but no SN Ia has yet been detected in the radio. However, the mass-loss limits derived via radio nondetections (*47, 56*) do not generally constrain RS Oph-like systems which has a mass-loss rate of $\sim 3 \times 10^{-7}$ $\mathrm{M_\odot}$ $\mathrm{yr^{-1}}$. Moreover, theory and observations suggest that the CSM distribution in symbiotic novae is nonuniform and the expected radio emission taking this into consideration has not yet been modeled. It is therefore unclear what effect this has on the limits derived from nondetection, but it is plausible that this would introduce a viewing-angle dependence that would decrease the chance for detecting the radio signal.

S7. Hα and Ca II Fluxes

Starting with the day $+39$ spectrum, a broad component of the Hα emission begins to appear; the profile can be decomposed into broad and narrow components. The full width at half-maximum intensity (FWHM) and the integrated fluxes in the broad component are given in Table S3. Starting with the day $+56$ spectrum, the Ca II emission begins to have a Gaussian appearance and the residual absorption seen in earlier spectra appears to be gone. The FWHM

and the integrated fluxes in the Ca II H&K lines are given in Table S4. To derive these values, the spectra were first spectrophotometrically calibrated to the r-band photometry from the Faulkes 2 m telescope. The Gaussian components of the emission feature were then fit using the deblending function in the `iraf splot` procedure.

S8. Mass Estimates

In the near-maximum-light spectra, the equivalent widths of the Ca II H&K lines are $\sim$ 10 Å. The lines are saturated, and on the square-root portion of the curve of growth, so that the equivalent width, W_λ, is given by

$$W_\lambda = (N \frac{\lambda_0^4}{2\pi c} \frac{g_u}{g_l} A_{ul} \gamma_u)^{1/2}, \tag{1}$$

where N is the column density, λ_0 is the wavelength of the transition, A_{ul} is the Einstein spontaneous emission coefficient, γ_u is the radiation damping constant, and g_u and g_l are the statistical weights of the upper and lower states, respectively. For the Ca II K line, with $\lambda_0 = 3933.6$ Å, this results in $N = 4.44 \times 10^{16} W_\lambda^2$ cm^{-2}. Thus, the column density in Ca II is $\sim 5 \times 10^{18}$ cm^{-2}. We write the total Ca mass as $M_{\mathrm{Ca}} = k \times 4\pi r^2$, where r is the radius at which the material exists and k is the covering fraction. The radius, r, can be estimated from the velocity of the SN ejecta, which we take to be $v \approx 25{,}000$ km s^{-1}, and the time at which the Ca goes into emission, which is $\sim +59$ days after explosion. This results in

$$M_{\mathrm{Ca}} = 3.43 \times 10^{-4} \, k \, (\frac{v}{25{,}000 \text{ km s}^{-1}} \frac{t}{59 \text{ days}})^2 (\frac{N}{5 \times 10^{18} \text{ cm}^{-2}}) \text{ M}_\odot. \tag{2}$$

Assuming a solar composition for the CSM, a value of $k = 1$ would imply a total mass in the CSM shell of ~ 5.3 M$_\odot$. Modeling of the light curve for the CSM SNe 1997cy and 2002ic results in an estimate of the mass in the CSM for those SNe of several solar masses (*22*).

The total luminosity of PTF 11kx is much less, and the decline rate much greater than that of either SN 1997cy or SN 2002ic, implying that the total CSM mass is also much less. Thus, we conclude that $k \ll 1$, and that the CSM material that generates the Ca II absorption is not uniformly distributed.

UT Date	Exposure Time (s)	SN Phase (days)	Wavelength Range	Median S/N	R ($\lambda/\Delta\lambda$)
20110128	1000	-1	3682-6538	10.4	48000
20110207	1800	+9	4017-8564	6.2	48000
20110218	1800	+20	3682-7993	3.5	48000
20110314	3600	+44	3682-7992	4.2	48000

Table S1. Journal of high-resolution spectroscopic observations. All spectra were taken with the HIRES instrument (57) on the Keck I telescope.

UT Date	Telescope	SN Phase (days)	Wavelength Range (Å)
20110126	Lick 3m	-3	$3448 - 10142$
20110128	Palomar 200in	-1	$3490 - 9750$
20110202	Lick 3m	+4	$3440 - 9754$
20110203	KPNO 4m	+5	$3487 - 7570$
20110209	Lick 3m	+11	$3430 - 10138$
20110221	WHT	+23	$3190 - 9279$
20110227	Lick 3m	+29	$3400 - 10000$
20110309	Keck1	+39	$3330 - 10188$
20110312	Keck1	+42	$3948 - 6128$
20110326	Keck1	+56	$3125 - 10233$
20110402	Gemini North	+63	$3815 - 9701$
20110411	KPNO 4m	+72	$3450 - 8451$
20110427	Keck1	+88	$3100 - 10200$
20110608	WHT	+130	$3036 - 9499$

Table S2. Journal of low-resolution spectroscopic observations.

UT Date	SN Phase (days)	σ_v (km s^{-1})	Flux (ergs s^{-1})
20110309	+39	600	1.64e+39
20110326	+56	980	4.36e+39
20110402	+63	1050	4.60e+39
20110427	+88	1590	1.84e+40
20110608	+130	2040	1.29e+40

Table S3. Hα velocity dispersion and integrated flux values.

UT Date	SN Phase (days)	CaII K σ_v (km s^{-1})	CaII K Flux (ergs s^{-1})	CaII H σ_v (km s^{-1})	CaII H Flux (ergs s^{-1})
20110326	+56	780	4.56e+39	610	2.75e+39
20110402	+63	680	2.56e+39	380	1.10e+39
20110427	+88	850	4.42e+39	970	2.72e+39

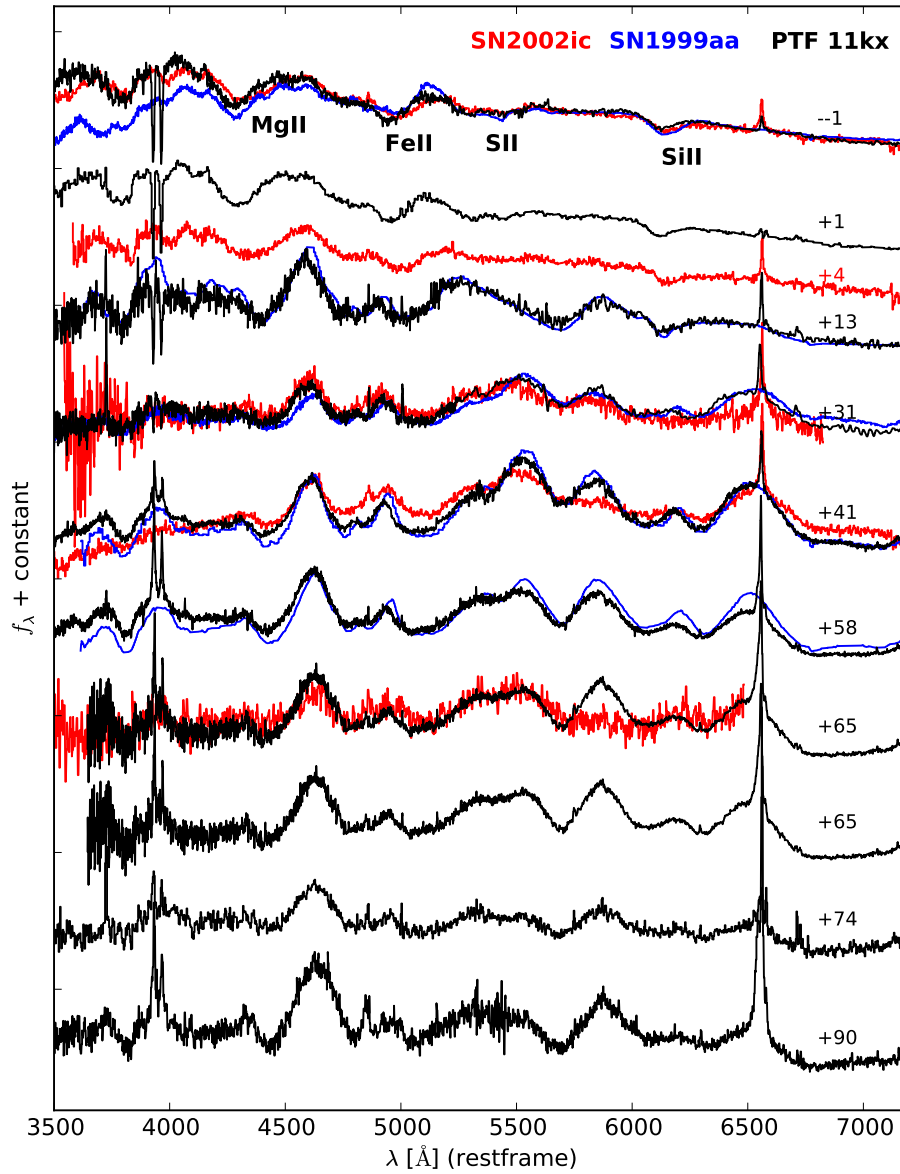Table S4. Ca II H & K velocity dispersions and integrated flux values.

Figure 1: **Comparison of spectra.** A temporal series of spectra of PTF 11kx is compared with that of the broad/bright SN 1999aa (*7*), and the CSM-interaction SN Ia, SN 2002ic (*16*), all at a similar phase. The location of Mg II, Fe II, S II and Si II present in the SN ejecta are labeled. The presence of both Si II and S II is a feature seen uniquely in SNe of Type Ia.
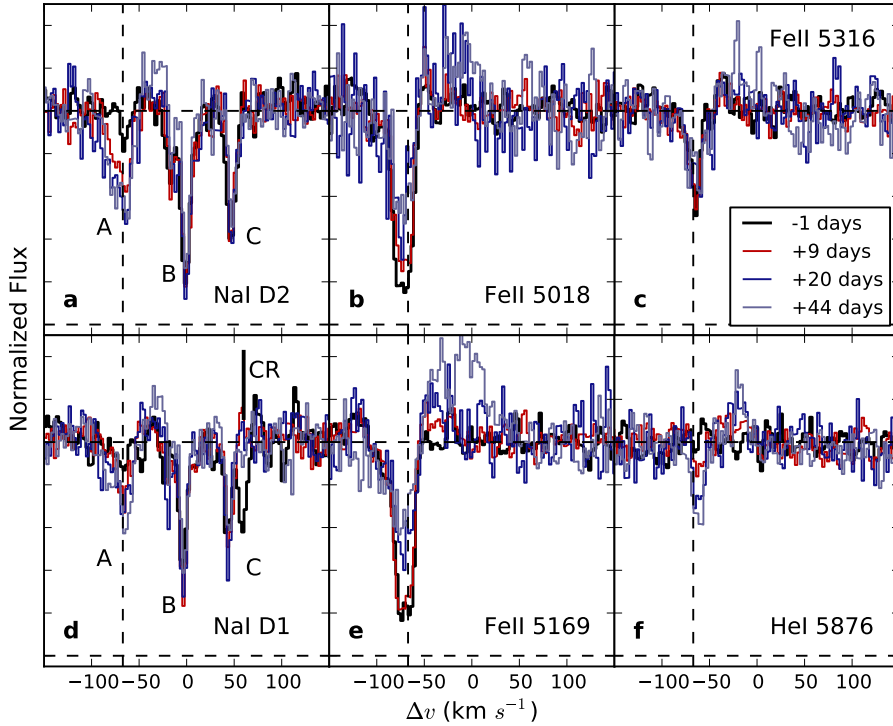
Figure 2: **The temporal evolution of narrow absorption features in PTF 11kx.** The panels show (a) Na I D2 , (b) Fe II $\lambda5018$, (c) Fe II $\lambda5316$, (d) Na I D1, (e) Fe II $\lambda5169$, and (f) He I $\lambda5876$. Separate components of Na I D are labelled as A, B, and C. Component A strengthens with time and is interpreted as ionization from the SN followed by recombination, and thus is from circumstellar material. Components B and C are attributed to the interstellar medium. The velocities are given relative to component B, which is taken as indicative of the local velocity of the SN progenitor system. The lower excitation states of Fe II (panels (b) and (e)) are seen to vary with time, while the higher excitation Fe II line (panel (c)) appears to be constant in time. He I absorption emerges in the later spectra. The vertical dashed line marks the velocity of the circumstellar material at -65 km s^{-1}. The horizontal dashed lines mark 1 and 0 in normalized flux units. A cosmic ray in the day -1 spectrum near Na I D1 is marked by "CR"; it produces a spurious absorption feature near the C component.
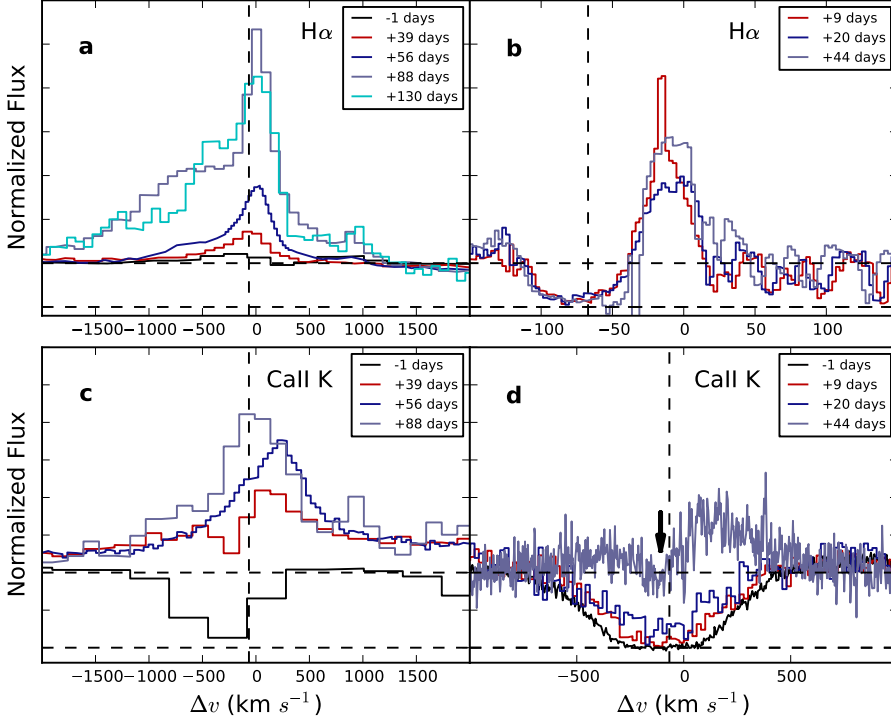
Figure 3: **The temporal evolution of Hα and Ca II K features in PTF 11kx.** (a) Low-resolution Hα, (b) high-resolution Hα, (c) low-resolution Ca II K, and (d) high-resolution Ca II K. The $+9$ and $+20$ day high-resolution Ca II spectra have been rebinned to 20 km s^{-1} precision for clarity of presentation. The vertical dashed line marks the velocity of the slower circumstellar material at -65 km s^{-1}. The large optical depth in the Hα line causes an apparent blueshift in the absorption minimum, relative to the -65 km s^{-1} expansion velocity of the narrow lines shown in Fig. 2. The horizontal dashed lines mark 0 and 1 in normalized flux units and show that at early times the Ca II lines are saturated. Narrow absorption, indicated by an arrow, can be seen superposed on the broad emission in the day +44 spectrum in panel (d). Narrow interstellar lines of Ca II, corresponding to components B and C in panels (a) and (d) of Fig. 1, can be seen at 0 km s^{-1} and $+45$ km s^{-1}. Several spectra in (a) and (c) appear to show narrow absorption superposed on broad emission, although the absorption is not always resolved. This indicates that, subsequent to the onset of CSM interaction, slower-moving material external to the inner shell of interacting material remains, possibly due to a decelerated nova shell.
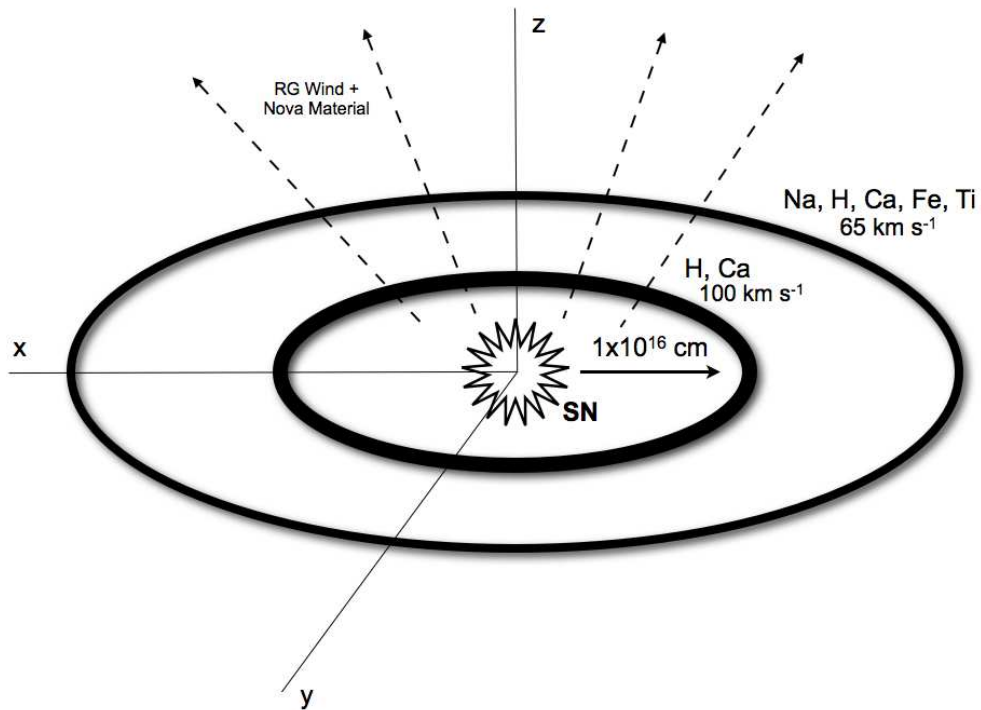
25

Figure 4: **Schematic showing the interpretation of the observations of PTF 11kx.** In the symbiotic nova progenitor system, a red giant wind deposits CSM into the system which is concentrated in the orbital plane. Episodic nova events further shape the CSM, resulting in expansion velocities of ~ 50–100 km s^{-1}. There is an inner region of material containing at least H and Ca, moving at ~ 100 km s^{-1}, surrounded by more distant material containing H, Ca, Na, Fe, Ti, and He, moving at ~ 65 km s^{-1}. The presence of hydrogen in the inner region is inferred from the onset of emission, concurrent with the onset of Ca II emission. This geometry, and the delay in the onset of CSM emission, is consistent with a relatively recent nova whose ejecta are sweeping up the circumstellar material and decelerating. The inner boundary of CSM is at a distance of $\sim 10^{16}$ cm, as determined from the onset of interaction.
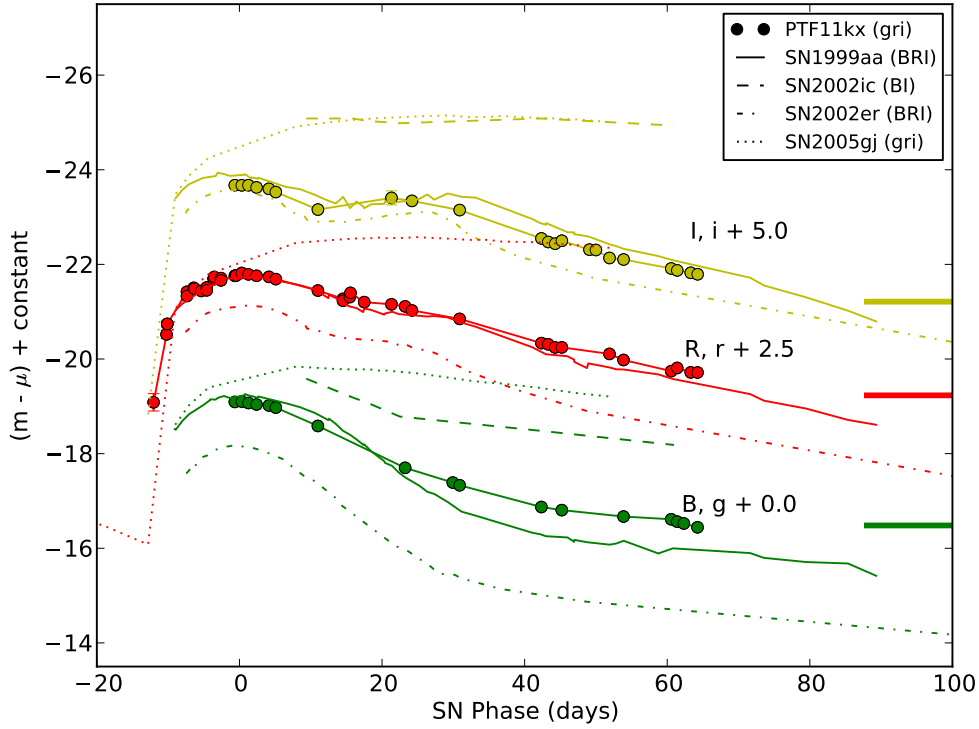
Figure S1: Comparison of the preliminary light curve of PTF 11kx to that of other SNe Ia. The data are the observer-frame magnitudes, without K-corrections. The PTF 11kx and SN 2005gj photometry is given in gri, and the other SNe in some combination of BRI. The red, green, and yellow points denote B/g, R/r, and I/i, respectively. The broad/bright SN 1999aa (solid) and the "normal" SN 2002er (dash-dot) are shown for comparison. Also shown are the CSM-interaction SNe Ia 2002ic (dashed) and 2005gj (dotted). PTF 11kx is much fainter than SN 2005gj and SN 2002ic, indicating a weaker/later onset of CSM interaction. The late-time, approximately constant, brightness of PTF 11kx is marked by the horizontal lines on the right side of the figure. Spectroscopically and photometrically, PTF 11kx bridges the observational gap between SN 1991T/SN 1999aa and SN 2002ic/SN 2005gj.